ISSN impresa 0717-3644
ISSN online 0718-221X

Maderas. Ciencia y tecnología 2024 (26): 49, 1-15

DOI: 10.22320/s0718221x/2024.49

EXPERIMENTAL AND NUMERICAL STUDY ON MOUNTING FORCE AND WITHDRAWAL STRENGTH OF SELF-THREADED DOWELS IN PARTICLEBOARD

Tolga Kuşkun [1,♠]

https://orcid.org/0000-0001-6657-139X

ABSTRACT

Traditional and alternative joining techniques have been used for many years at the connection points of structural bearing systems. Especially, glued doweled and screwed type mechanical connections are widely used in wooden structures and furniture constructions. Although there are many studies related to the strength of dowel and screw joints, limited papers describe the practical use of self-threaded dowels (STDs) in the joints. In this study, thread geometry effect of the STDs in particleboard (PB) was investigated by determining the mounting force and withdrawal strength values. For this purpose, STDs including three different thread width (0,2 - 0,3 - 0,4 mm) and two different thread length (1 - 2 mm) were designed, produced and tested under static compressive and tensile forces. All STDs were produced with polylactic acid (PLA) by using Layer Plastic Deposition (LPD) method in 3D printing technology. Uniaxial compression tests were performed in order to determine the minimum mounting force while the tension tests were performed for determining the maximum withdrawal force required to put the STDs into the hole and pull out them, respectively. Numerical analysis (FEM) were used to analyze the contact pressures and stresses of the STD joints. Abaqus v6.13-1 software was utilized for the numerical analyses. In addition, multiple regression analysis was carried out to predict the mounting force and withdrawal strength of the STDs. Results showed that the predictive expressions developed provided reasonable estimates for mounting force and withdrawal strength of STDs. According to the statistical analyses; thread width, thread length and their interaction have significantly affected both mounting force and withdrawal strength of STDs. At the end of the experimental and numerical tests, STDs with 0,2 mm width and 2 mm length threads gave the lowest mounting force values, stresses and contact forces. However, the highest withdrawal strength values were obtained from the STDs with 0,3 mm width and 1 mm length threads. According to the results of the study, the optimum STD was the one with 0,3 mm thread width and 2 mm thread length. In conclusion, the STDs can be utilized as an alternative fastener to the conventional glued dowel type joints in PB. However, corner joints constructed of different kinds of wood-based composites and connected with the STDs should be investigated in the future studies.

Keywords: Furniture constructions, wooden structures, Wood-based composites, numerical analyses, self-threaded dowel, withdrawal strength.

INTRODUCTION

Traditional joints such as glued dowel and screw types connections are widely use in wooden structures and furniture constructions. Those connectors are commonly used in structures constructed of wood based composite materials. However, connection types like screw have disadvantage such as some extra equipment for mounting and also dowel connections can't be produce without glue. Both connection types need more time and application schedule.

Zhang *et. al.* (2016) investigated the thread configuration of self-tapping screws for timbers, and indicated that the efficiency of screw reinforcing was affected by thread configuration.

Smardzewski and Ozarska (2005) created a numerical model of cabinet furniture assembly using confirmat-style semi-rigid screw joints as well as a mathematical model of a semi-rigid angle joint. It was demonstrated that models of a confirmat type semi-rigid constructional node accurately represent the operation of a stiff connection in close proximity of strongly deformable wood-derived materials. The authors have developed a mathematical and numerical model of a confirmat-type semi-rigid angle joint loaded with a bending moment.

[1]Muğla Sıtkı Koçman University. Faculty of Technology. Department of Woodworking Industrial Engineering. Muğla, Turkey.
[♠]Corresponding author: tolgakuskun@mu.edu.tr
Received: 22.12.2023 Accepted: 15.09.2024

Using a range of mostly screw-based fasteners, the ability to join 15,87 mm thickness of furniture particleboard was tested. Independent statistical tests were performed to specify the effects of screw diameter, screw head, screw thread shape, and fastener type (dowel, screw + PVC anchor, or screw) on edge screw withdrawal strength, corner joint bending moment resistance, and lateral edge load of butt-jointed shelf units. The edge screw withdrawal resistance and bending moment resistance were greatly enhanced with a thicker diameter (6,4 mm), although the edge load of shelf joints was higher with thinner screws. The screws with a fully threaded shank performed best in the lateral edge load testing, and 9 threads per inch yielded the maximum edge screw withdrawal resistance. In all three tests, replacing screws with an unglued dowel connection or a big expandable PVC anchor decreased the performance of the fasteners (Park *et al.* 2006).

Another connection type commonly used in constructions is dowel joints. In such traditional connection methods, expertise and time are required to apply the glue and achieve proper joint. Due to its ease of manufacture and low cost, the dowel joint is a commonly used connection method in furniture products and building construction, among other things. Quantitative research was done on the influence of dowel placement, dimension, and loading distance on bending moment capacity. Usually, rather than the composite itself, it is the connections between each component that lead to the breakdown of the entire building (Chen *et al.* 2017, Hao *et al.* 2020). The dowel and board member with holes should have the proper interference fit to secure the connection firmly (Mougel *et al.* 2011, Wang and Lee 2014).

A study of Hao *et al.* (2020) included the development of a mathematical model to predict the bending moment resistance of various dowels. Therefore, strengthening dowels, lengthening them, enlarging the dowel gap, and relocating the bottom dowel away from the bottom edge will all enhance joint performance. It should be remembered that the ideal joint properties are determined by the ratio of dowel diameter to length, which is two times that of dowel withdrawal strength to dowel tensile strength (Hao *et al.* 2020). The bending moment capacity or stiffness of the dowel joint gradually increased with increasing dowel diameter and length (Chen *et al.* 2018, Hao *et al.* 2020, Norvydas *et al.* 2005, Sawata and Yasumura 2002, Zhang and Eckelman 1993).

The withdrawal force capacity of T-type corner joints made from medium density fiberboard (MDF) and particleboard (PB) constructed with various sizes of beech dowels is calculated using predictive expressions developed by Yüksel *et al.* (2022). The effects of material type, dowel diameter, penetration, and adhesive type on withdrawal force capacity were also examined. Statistics have shown that the type of material, dowel diameter, penetration, adhesive type, and their four-way interaction have a significant impact on the withdrawal force capacity of dowels. MDF with PU adhesive achieved the maximum withdrawal force capacity among the adhesive and material. The penetration or dowel diameter was increased, which increased the withdrawal force capacity. The capacity for withdrawal force was found to be less affected by dowel penetration than by dowel diameter (Yüksel *et al.* 2022).

The construction and furniture industries are utilizing Additive Manufacturing (AM), commonly known as 3D printing, in new types of structures and fasteners (Ho *et al.* 2015, Kuşkun *et al.* 2021). Three-dimensional printing, also referred to as additive manufacturing, is a modern manufacturing process (Lukic *et al.* 2016). It combines standardized materials and specified automatic processes to create customized 3D objects based on digital computer-aided design (CAD) models (Lin *et al.* 2019, Vukicevic *et al.* 2017). It is used for rapid prototyping, which has been popularized in the manufacturing, engineering, design, and industrial sectors for about 30 years. Due to the quick development of new materials, printing technology, and tools, established methods of experimentation and education are expected to be drastically changed by 3D printing (Gross *et al.* 2014). Traditionally, manufacturing processes employed in industries involved carving out designs from a solid block of material. In contrast, the layer-by-layer method used in additive manufacturing enables more complex designs and interior models (Kuşkun *et al.* 2021, Su and Al'Aref 2018). In this study, 6 different types self -threaded dowels (STD) were produced by using 3D printing Layer Plastic Deposition (LPD) technology.

By using solid modeling and structural analysis software, construction engineering designs can be completed. The easiest way for assessing structural systems is to use finite element methods (FEM). Through the use of FEM, structural members, joints, and the whole system can be parametrically modelled. Because of the tools offered by solid modeling, modifications can be made realistically and the revised design of the system can be compared to the original, even though a small change during the design phase can have a significant impact on the system as a whole. As a result, the ideal solution can be found (Kasal *et al.* 2016).

The effects of tenon length on the flexibility of mortise and tenon joints were numerically analyzed in the study by Hajdarević and Martinovic (2014). Results showed that as tenon length increased, mortise and tenon joints were stiffer. The findings also demonstrated that the deflection of a structure was significantly influenced by the stiffness of the joints in a frame (Hajdarević and Martinović 2014).

It can be seen that traditional joining techniques such as glued dowel, glued mortise and tenon or mechanical fasteners that provide portable connections are generally used in furniture joints for both case and frame type furniture. Today, naturally, glued joints have been replaced by mechanical fastener joints due to

their advantages such as ease of storage, transportation and assembly. However, problems are encountered with these fasteners, such as the excessive number of operations, the diversity of operations, and the fact that the assembling is not well understood and performed by the users. Accordingly, in this study, it is proposed to use the dowels with a self-threaded outer surface. In this context, the effects of the thread geometry on the outer surfaces of self-threaded dowels (STDs) on mounting forces and withdrawal strength will be investigated. As can be understood from the literature review, there are numerous studies linked to the dowel joints but limited numbers of papers describe the STDs performance. In this study six type of STD were produced and tested by determining the mounting force and withdrawal strength in PB. In the scope of the study, a total of 60 specimens (three thread width, two thread length, ten replications for each) were tested under compressive force and these specimens were then tested under tensile forces. In addition, multiple regression analysis was carried out to predict the mounting force and withdrawal strength of the STDs as a function of thread width and thread length. Finally, 6 type of connection were numerically (FEM) analyzed by using Abaqus v6.13-1 (Dassault Systemes Simulia Corp., USA, 2013) software in order to obtain contact pressures and stresses of the STD joints.

Materials and methods

Mechanical and elastic properties of STD and base materials

All dowels were produced by using polylactic acid (PLA). Before producing the dowels, mechanical and elastic properties of the PLA materials were determined. According to the ASTM D3039/D3039M-17 (2017) methods, the uniaxial static tensile tests were utilized to determine the mechanical and elastic properties of PLA. A total of 10 test samples were prepared with 3D printer and tested (Figure 1). Tensile tests were carried out on numerically controlled universal test machine with 10mm/min loading under static load. According to the results of the tensile tests, elasticity modulus (MOE) for PLA was equal to 796 MPa and tensile strength (MOR) was equal to 20 MPa.

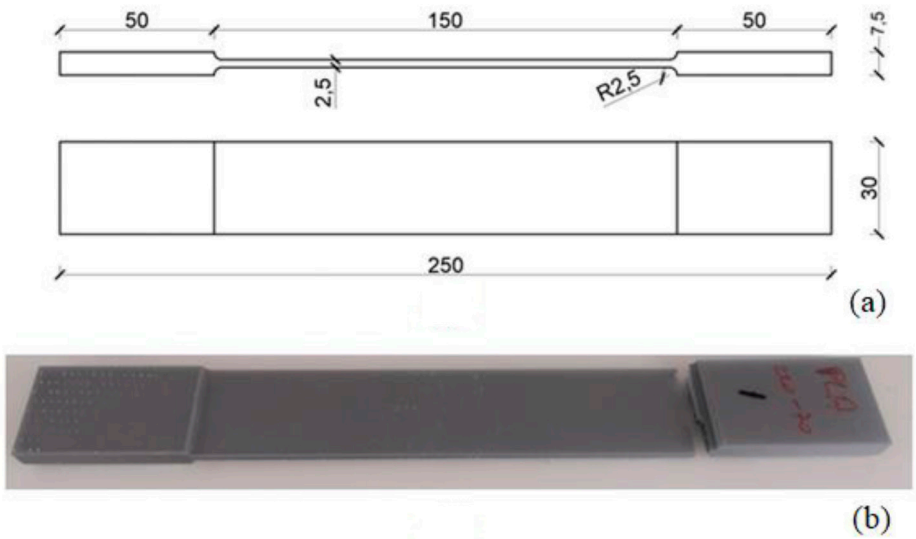

Figure 1: (a) Dimensions (Kuşkun *et al.* 2021) and (b) picture of the PLA tensile test sample.

The sample base material was 18 mm-thick particle board (PB) with a modulus of elasticity of 3660 MPa and modulus of rupture of 11,35 MPa.

Design and producing of the STDs

In the scope of the study, 6 different kinds of threads were designed and evaluated. All dowels designed were in 30 mm length and 10 mm diameter. Threads of dowels had 3 different sizes (0,2 - 0,3 - 0,4 mm) of width and 2 different sizes (1 - 2 mm) of length (Figure 2a, Figure 2b, Figure 2c, Figure 2d, Figure 2e, Figure 2f).

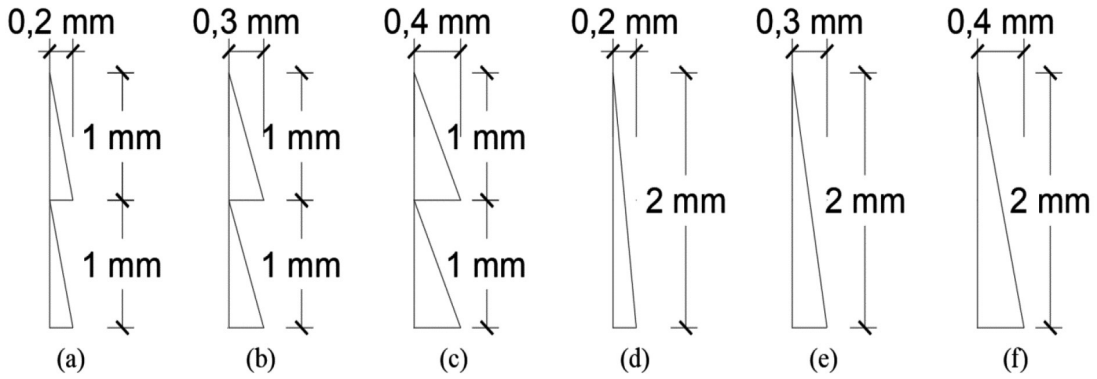

Figure 2: The shape and the dimensions of the thread. (a) 0,2 mm W – 1 mm L, (b) 0,3 mm W – 1 mm L, (c) 0,4 mm W – 1 mm L, (d) 0,2 mm W – 2 mm L, (e) 0,3 mm W – 2 mm L, (f) 0,4 mm W – 2 mm L of dowel threads (W: width, L: length).

All STDs are produced with 3D printer Layer Plastic Deposition (LPD) technology, with a 1-degree angle at the base of the screw thread. Thanks to this angle at the base of the dowel thread, production of STDs will be easier for the 3D printing. The use of LPD technology enables the construction of even extremely complicated joint prototypes with a high degree of material isotropy.

All produced dowels had a special head (22 x 22 x 8 mm rectangular box shaped) for easy application of the compressive and tensile force during the tests. 3D modelled STDs with each thread geometry are illustrated in the Figure 3a, Figure 3b, Figure 3c, Figure 3d, Figure 3e and Figure 3f.

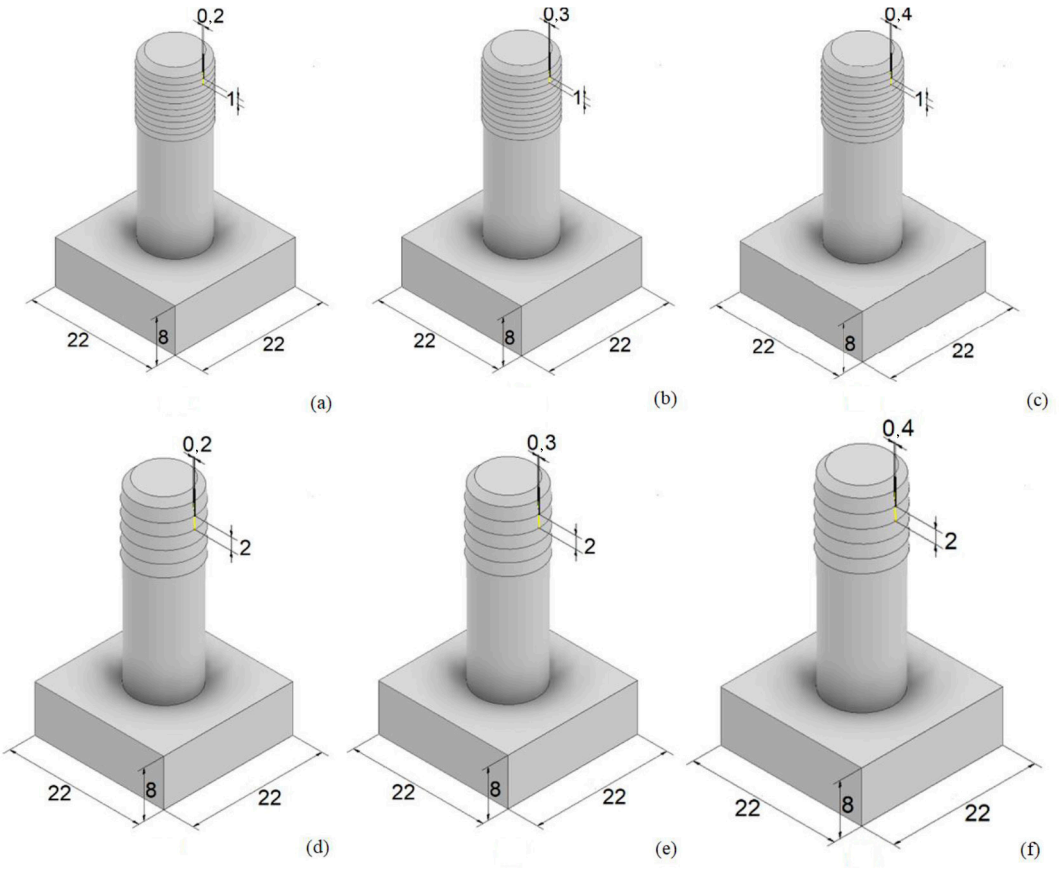

Figure 3: Models of dowels prepared for 3D printing. (a) 0,2 mm W– 1 mm L, (b) 0,3 mm W – 1 mm L, (c) 0,4 mm W – 1 mm L, (d) 0,2 mm W – 2 mm L, (e) 0,3 mm W – 2 mm L, (f) 0,4 mm W – 2 mm L of STD samples (W: width, L: length).

As seen in Figure 4, STD dowels with different size were produced and tested under mounting and withdrawal forces. Additionally, 6 different type of STD samples were evaluated and numerical analyzed by using Abaqus software.

Mounting force and withdrawal strength test sample configuration

70 x 70 mm square shaped samples were prepared of 18 mm thick PB for determining the mounting force and withdrawal strength of the STDs. In the study, no adhesive was used for the connection between the STDs and PB, and the STDs were connected to the PB materials only with the threads on their outer surface. Total of 60 mounting force test samples were prepared and tested under compression. Then, the same samples were tested under tension in order to determine the withdrawal strength of the STDs. The dimensions and general view of the test samples are shown in Figure 4a, Figure 4b.

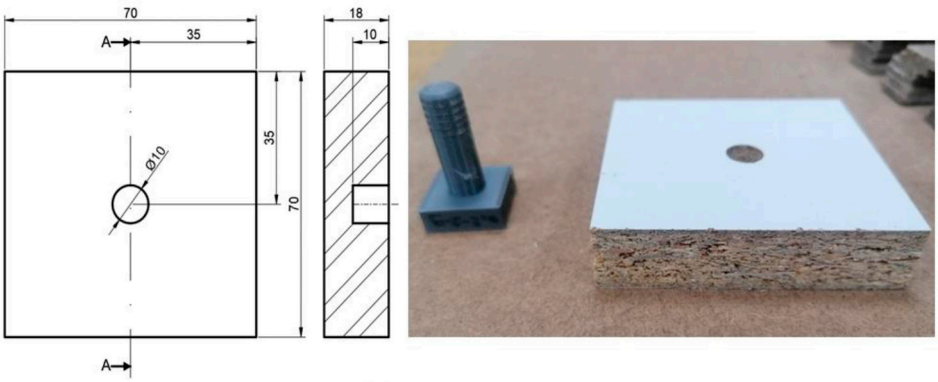

Figure 4: (a) Dimensions and (b) configuration of the test samples.

Numerical models of the samples

The mounting force test samples supported FEM models similarly to the actual test. Figure 5a served as a base for the model's geometry, loading, and boundary conditions. In the model, 10-node modified quadratic tetrahedron elements of type C3D10M were used (approximately 18000 elements and 29000 nodes per model) (Figure 5b).

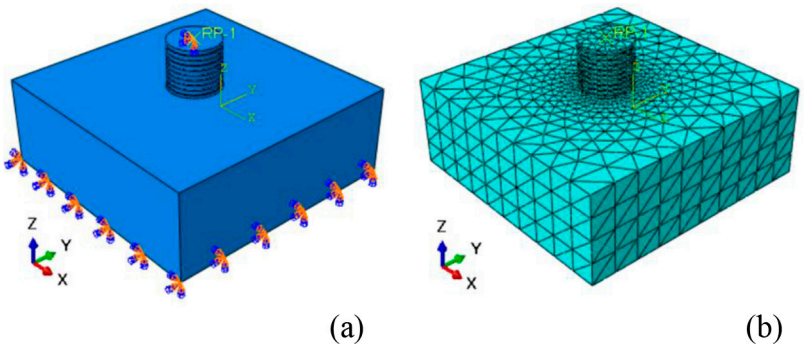

Figure 5: (a) Boundary condition and (b) mesh model of numeric analysis.

As seen in Figure 5a, Reference Point 1 (RP1) was added on the top of the STD. RP1 was connected with rigid connection to the top surfaces of STD, and 10 mm displacement from vertical (-Z) direction was applied. Fixed support was applied from the bottom surface of the PB. Between STD and PB general surface frictionless contact was modeled. The PLA an PB are modeled as elastic - isotropic material. Abaqus/Explicite v.6.13-1 (Dassault Systemes Simulia Corp., USA, 2013) was used to conduct the finite element analysis. Results of numerical computations were used to determine the contact pressures and contact stress levels of STD joints.

Mounting force and withdrawal strength tests

For all STDs mounting force and withdrawal strength tests, a numerically controlled universal testing machine with a 5 kN capacity and a 10 mm/min loading rate was utilized. Mounting force and withdrawal strength tests were performed under static uniaxial compression and tension loading, respectively. In the tests, dowels were inserted into the hole at the mounting force test (Figure 6a), and withdraw from the hole at the withdrawal strength tests (Figure 6b) on the 10 mm deep during the time period 60-90 s.

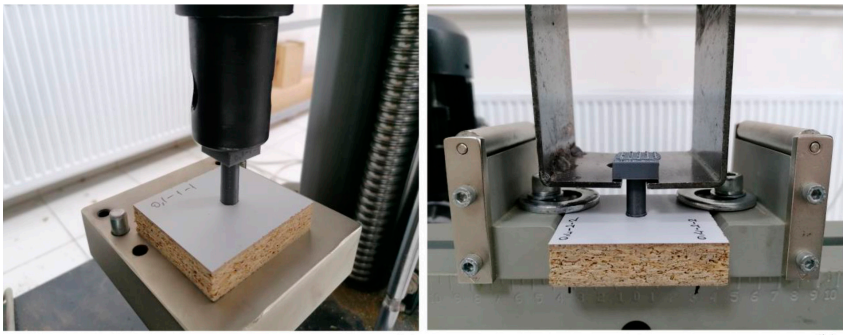

(a) (b)

Figure 6: Test setup for (a) mounting force, and (b) withdrawal test.

Produced dowels had a special head for easy application of the load. In order to mount and withdraw the dowel during testing, focused static vertical compression and tension loads were applied from the dowel head

Statistical analyses

The mounting force and withdrawal strength values obtained were examined by performing the two-way analysis of variances (MANOVA) general linear model approach in order to determine the effect of the two independent variables (thread width, thread length) and their interactions (thread width X thread length) on both mounting force and withdrawal strength. In order to take into consideration for the "thread type," which was statistically significant in the MANOVA results, the mounting force and withdrawal strength values of the tested samples were calculated using the Least Significant Difference (LSD) multiple comparisons approach at the 5 % significance level. In addition, multiple regression analysis was performed for predicting both mounting force and withdrawal strength values of the STDs connections with PB as a function of thread width and thread length. As a result, predictive expressions were developed and compared to the actual test results. For the statistical analysis, Minitab (Version 17) statistical software was used (Minitab 2023, LLC, State College, PA, USA).

Results and discussion

Failure modes for withdrawal tests

Two different type of failure modes were observed during the withdrawal tests. First type of failure was observed from the 0,2 mm width STDs regardless of threads length. In that failure type, dowels withdraw from the hole in PB without any deformation Figure 7.

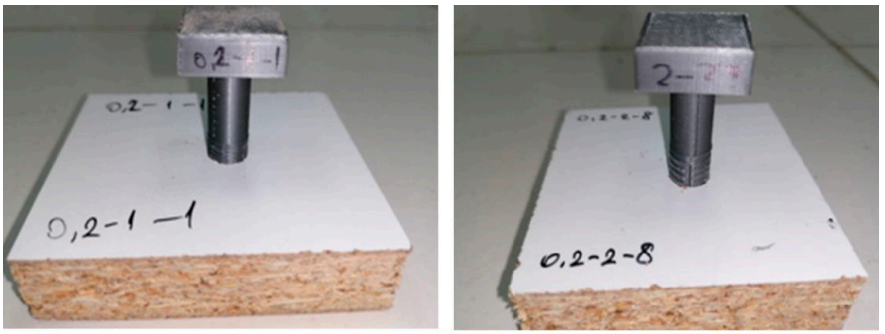

(a) (b)

Figure 7: Failure modes after withdrawal tests. (a) 0,2 mm W – 1 mm L, (b) 0,2 mm W – 2 mm L STD deformations (W: width, L: length).

This failure mode shows that the 0,2 mm thread depth is not sufficient for the STD to hold in the PB. For this reason, the STD could not hold on to the PB and withdraw directly without damaging the PB.

In case of the second type of failure mode, PB was failed by STD withdraw from the surface along with some base material together, with edge splitting of the PB. In another words, the surface of the PB swelled in the STD pulling area and edge splits occurred in transverse direction of the PB around the STD (Figure 8). This failure type occurred at 0,3 and 0,4 width thread, regardless of thread length.

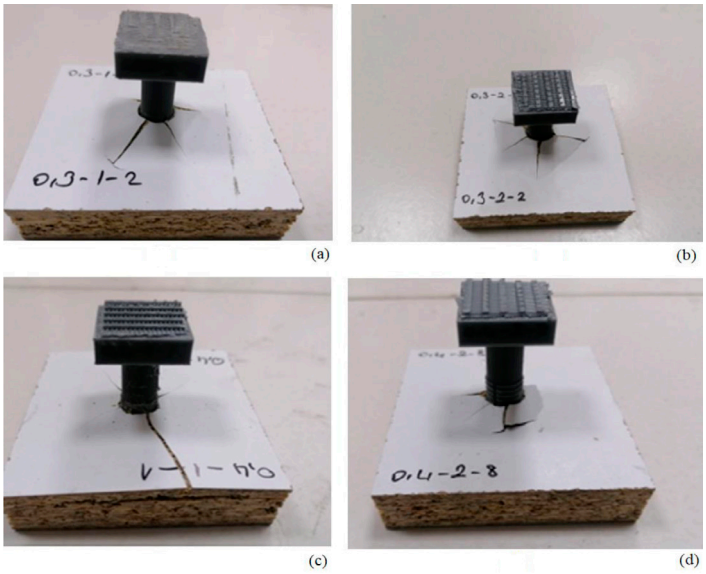

Figure 8: Failure modes after withdrawal tests. (a) 0,3 mm W – 1 mm L, (b) 0,3 mm W – 2 mm L, (a) 0,4 mm W – 1 mm L, (b) 0,4 mm W – 2 mm L STD deformations (W: width, L: length).

As a result of the applied tensile force, the STD held in the PB forced the board material in perpendicular to its surface direction. This force is also related to the internal bond strength (IB) of the PB. It is understood from the second failure mode type that increasing the tread width increases the holding strength, and the holding strength continues until the internal bond (IB) strength of the PB is exceeded.

Experimental results for mounting force and withdrawal strength

MANOVA results indicated that effect of the main factors (thread width and thread length) and their two-way interaction on mounting force values were statistically significant at the 5 % significance level. In case of the withdrawal strength, the effect of only one main factor (thread width) was found to be significant at the 5 % significance level. Table 1 presents the two-way analysis of variance results.

Table 1: MANOVA Results for mounting force and withdrawal strength values.

Source		Degrees of freedom	Sum of squares	Mean squares	F-Value	P-Value
Mounting Force	Thread Width	2	954692	477346	173,89	0,000
	Thread Length	1	59814	59814	21,79	0,000
	T. Width x T. Length	2	20761	10381	3,78	0,029
	Error	54	148238	2745		
	Total	59	1183505			
Withdrawal Strength	Thread Width	2	218114	109057	53,63	0,000
	Thread Length	1	3630	3630	1,78	0,187
	T. Width x T. Length	2	412	206	0,10	0,904
	Error	54	109814	2034		
	Total	59	331969			

Examination of F values shows that thread depth has a much greater impact on both mounting force and withdrawal strength than thread length. Table 2 compares the mean mounting force values according to the main factors.

Table 2: Main factor effects on the mean mounting force values.

Thread Width (mm)	Mean (N)	HG	Thread Length (mm)	Mean (N)	HG
0,2	454,53	A	2	585,19	A
0,3	633,62	B	1	648,33	B
0,4	762,13	C			

HG: Homogeneous Group.

Results indicated that the mounting force values of STDs increased when the thread width is significantly increased. The mean mounting force of 0,2 mm thread width STDs were the lowest mounting force and they were 30 % lower than 0,3 mm thread width STDs. In case of the STDs width 0,3 mm thread width, mean mounting force was lower than the mean values of STDs with 0,4 mm thread width by 17 %. Comparison results for the effect of thread length factor on the mounting force indicated that 2 mm length thread STDs gave the lower mounting force value by 10 % than the STDs with 1 mm thread length. In conclusion; it was observed that more mounting force was generated in the test samples with a 1 mm thread length STDs. This situation is revealed by the fact that the STDS with 1 mm thread length have higher contact surfaces between the intersection areas of threads and inner walls of hole in PB. In another words; the contact of more threads with the inner surface of the hole drilled into the PB in 1 mm thread length increased the friction and therefore mounting force.

Table 3 gives mean comparisons of mounting force values of the thread width x thread length two-way interaction.

Table 3: Mean comparison for thread width x thread length interaction for mounting force.

Thread Width (mm)	Thread Length (mm)			
	1		2	
	Mean (N)	HG	Mean (N)	HG
0,2	509,03	B	400,03	A
0,3	664,90	D	602,33	C
0,4	771,07	E	753,19	E

As seen in Table 3, the STDs with 0,2 mm thread width and 2 mm thread length gave the lowest mounting force values. The highest mounting force values were obtained from the STDs with 0,4 mm thread width and 1 mm thread length. Overall, it could be said from the results that for low mounting force, it is necessary to use small thread width and large thread length for the STDs. However, low mounting force in itself is not a very meaningful indicator. In addition to the mounting force, the withdrawal strength of the STD should also be evaluated, and the higher one should be preferred.

Mean comparison results for the thread width of the STD which was found statistically significant in the MANOVA for withdrawal strength was given in the Table 4.

Table 4: Mean comparison of thread width for withdrawal strength.

Thread Width (mm)	Mean (N)	HG
0,4	604,02	A
0,3	599,99	A
0,2	474,15	B

According to Table 4, STDs with 0,2 mm thread width gave the lowest withdrawal strength while the highest withdrawal strength values were obtained from the STDs with 0,4 mm thread width. Accordingly, increasing the thread width significantly increased the withdrawal strength of STDs.

The experimental force-displacement relationships of the STDs under the withdrawal force are given in Figure 9.

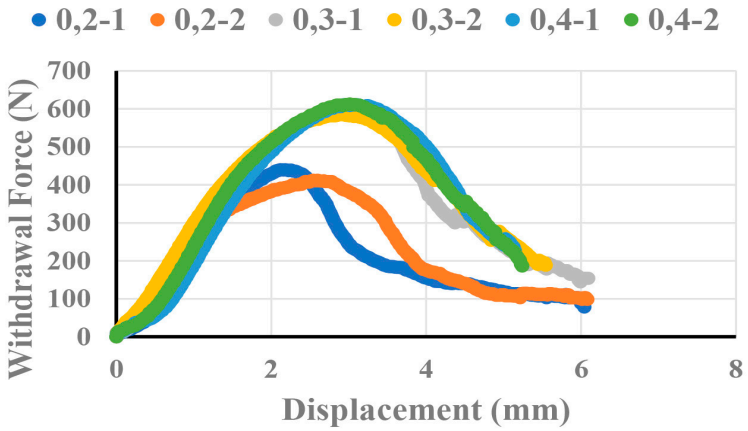

Figure 9: Force-Displacement relation of withdrawal tests for STDs.

As shown in Figure 9, specimens with a thread width of 0,2 mm gave lower values, while the other four groups gave higher and closer values. In STDs of 0,3 mm and 0,4 mm width, the maximum withdrawal capacity averages 600 N, with a deformation of around 3 mm. According to the force-displacement relationships, mechanical behavior of the STDs was observed similarly for all groups. In all types of STD, the withdrawal force increased linearly up to a certain point, then turn into a into a parabolic behavior, reaching the maximum value (3 mm for the STDs which have 0,3-1; 0,3-2; 0,4-1; 0,4-2 threads; approximately 2,5 mm for the STDs which have 0,2-1; 0,2-2 threads), and then decreased and finally failed. Generally, the consistent mechanical behavior results were obtained with the failure modes of the STDs. As can be clearly understood from the failure modes of the STDs (0,3-1, 0.3-2, 0,4-1, 0,4-2), which rupture the material as they withdraw from the material, they hold on to the material much better and therefore carry relatively more withdrawal force. As for the remaining STDs (0,2-1, 0,2-2), which have a failure mode of withdraw directly from the material, it can be said that they cannot hold on to the material sufficiently and therefore fail at relatively lower withdrawal forces.

As mentioned before, the mounting forces and withdrawal strength of the STDs should be evaluated together. In this context, the optimum STDs tested within the scope of this study are those with 0,3 mm thread width and 2 mm thread length.

Results of numerical analyses

Contact pressures around the surface of STDs and contact stresses for the PB were evaluated during the mounting with numerical analysis. According to the results of numerical analyses, the highest contact pressures and stresses were obtained from the STDs with 0,4 mm thread width and 1 mm thread length.

At the end of the analyses results obtained for the contact pressures, it could be noticed that as the thread width increased, the contact pressures also increased. The lowest contact pressure around the surface of STDs was obtained as 13,28 MPa from the STD with 0,2 mm thread width and 1 mm thread length. The highest contact pressure around the surface of STDs was obtained as 40,02 MPa from the STD with 0,4 mm thread width and 1 mm thread length. All contact pressure values obtained from the numerical analyses were given in Figure 10.

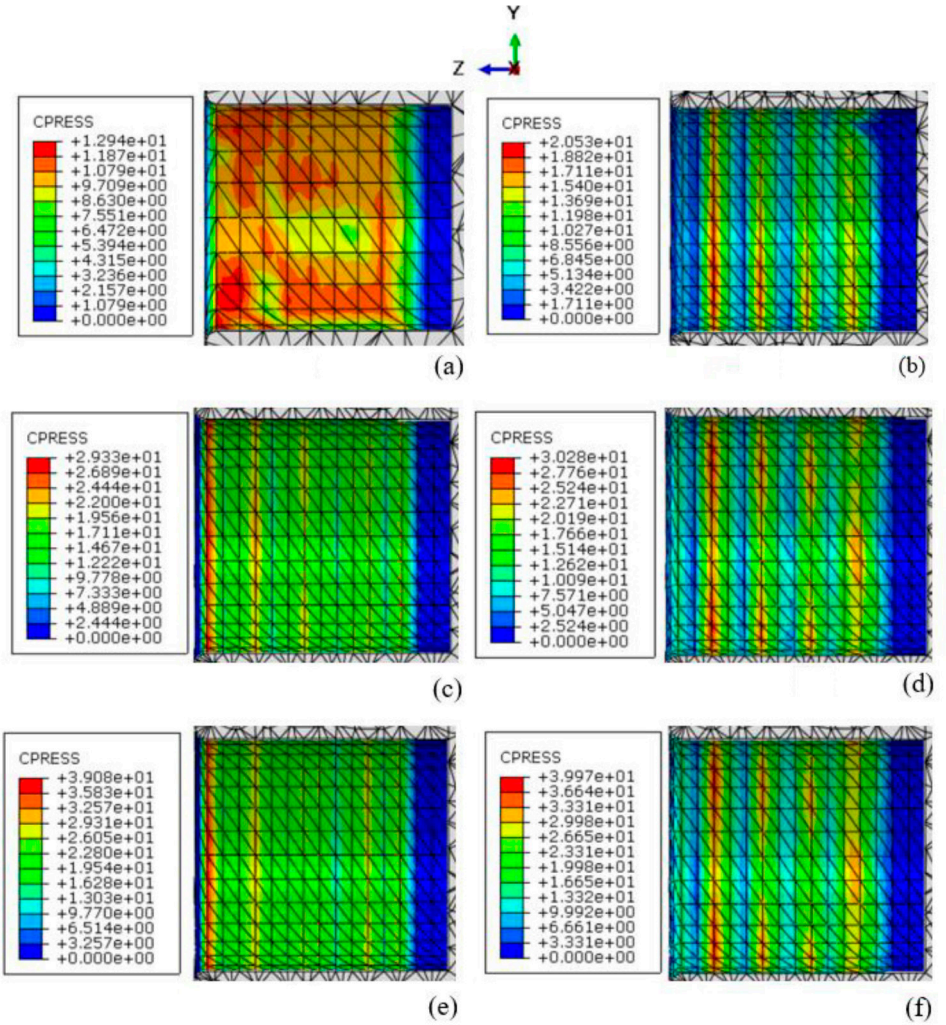

Figure 10: Contact pressures around the surface of STDs under the mounting test. (a) 0,2 mm W – 1 mm L (b) 0,2 mm W – 2 mm L (c) 0,3 mm E – 1 mm L (d) 0,3 mm W – 2 mm L (e) 0,4 mm W – 1 mm L (f) 0,4 mm W – 2 mm L (W: width, L: length).

All contact pressure was given at the highest value for the mounting tests. As seen in Figure 9a, during the mounting of threads with 0,2 mm width – 1 mm length STD reached 12,94 MPa contact pressure. That value is the minimum contact pressure value among the all specimens. Highest contact pressure value was obtained from the 0,4 mm width – 2 mm length STD was 37,97 MPa (Figure 10f).

STDs with 0,2 mm width has lowest contact pressure and highest contact pressures were obtained from STDs with 0,4 mm width. It can conclude that form the results STDs contact pressures were increased while thread size of STDs increased. Additionally, it is seen that load concentrations occur as the thread length increases. This occurs because the 2 mm long thread lengths are fewer in the hole in the PB. In other words, since the 1 mm thread length are more in the 10 mm hole and cover more area, it can be seen that the contact pressure on the STDs with 1 mm thread length are distributed more homogeneously on the surface of the hole.

The maximum Mises stress distribution within PB during the mounting procedure was obtained from the numerical analyses results, and the graphical results are shown in Figure 11. According to the results, it could be concluded that as the thread width increased, the contact stress also increased.

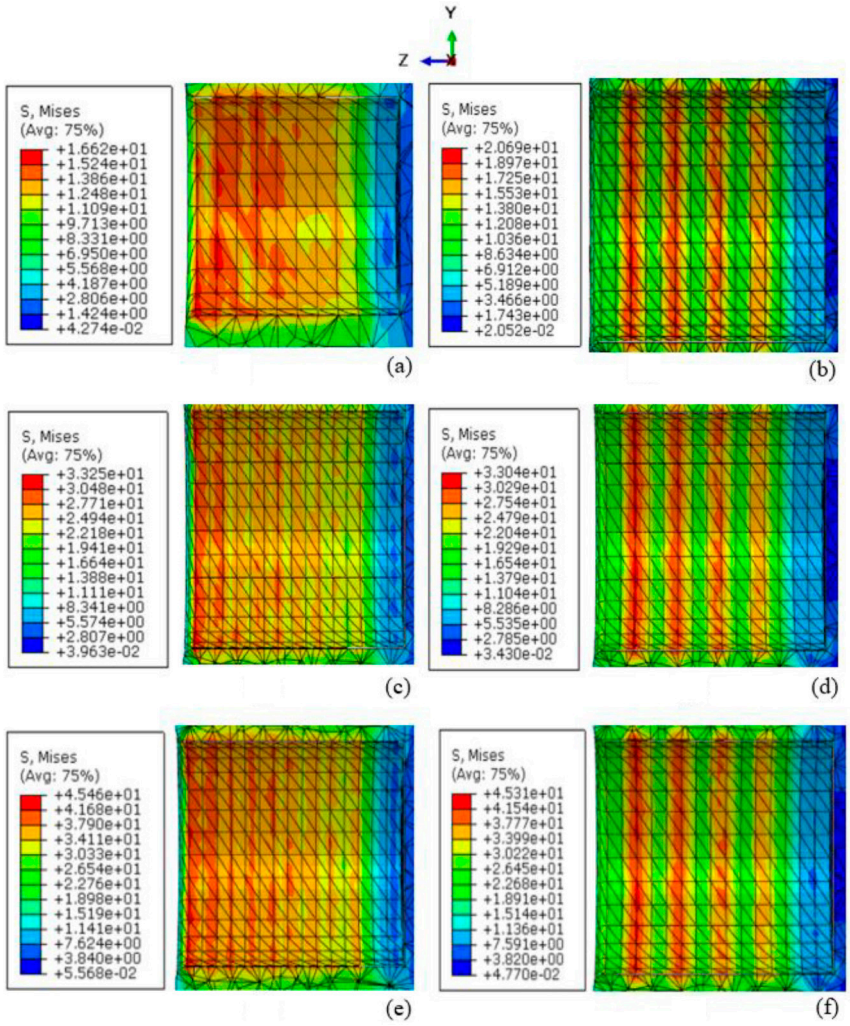

Figure 11: Contact stresses in the PB under the mounting test. (a) 0,2 mm W – 1 mm L (b) 0,2 mm W – 2 mm L (c) 0,3 mm E – 1 mm L (d) 0,3 mm W – 2 mm L (e) 0,4 mm W – 1 mm L (f) 0,4 mm W – 2 mm L (W: width, L: length).

As seen in Figure 11, with the effect of mounting force, the stresses inner surface of the PB increased while STD thread width increased. All contact stress levels were given at the highest value for the PB. During the mounting of threads with 0,2 mm width – 1 mm length STD reached 16,62 MPa contact stress. That value is the minimum contact stress among the all specimens. Highest contact stress value was obtained from the 0,4 mm width – 1 mm length STD was 45,46 MPa (Figure 11f).

The stress distributions and contact pressures are consistent with each other. When the stress distributions are examined, stresses increased as the thread width increased, and stress concentrations occurred as the thread length increased. As the screw width increased, the stresses on the PB increased and it became difficult for the STDs to withdraw from the hole. When thread lengths were examined, it was seen that, as in the contact forces section, 1 mm long screw stresses were more homogeneously distributed and there were stress concentrations in 2 mm long screws. When the thread lengths were examined, it was seen that as in the contact forces section, the stresses created by 1 mm thread lengths in the PB were more homogeneously distributed and 2 mm long screws had stress concentrations in the PB. This situation is explained by the fact that the contact areas are larger in 1 mm long screws.

The changes in contact pressures and stresses on the inner surface of the hole in the particleboard during the mounting test are shown in Figure 12.

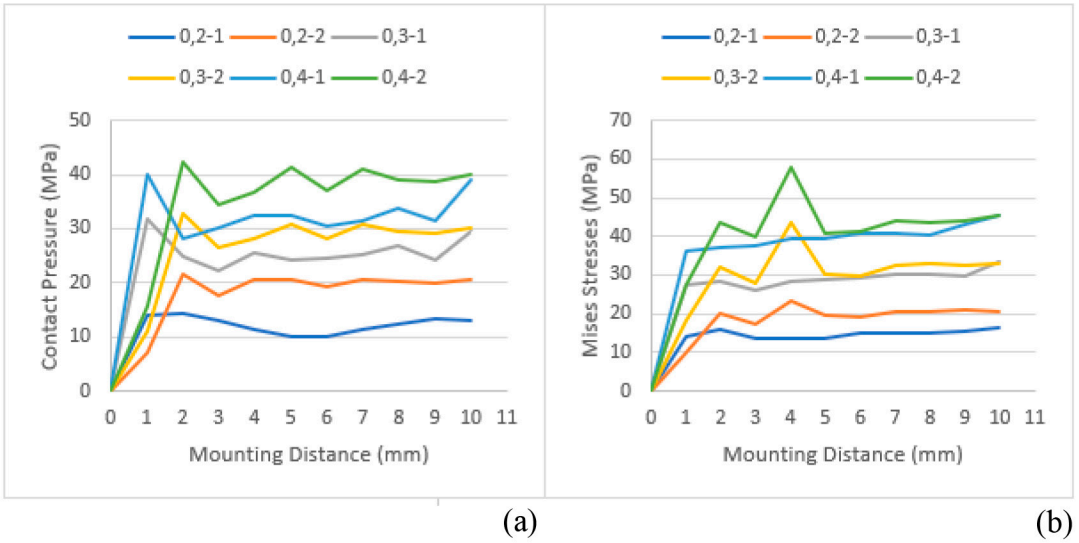

Figure 12: (a) Contact pressures and (b) contact stresses during the mounting test.

As seen in Figure 12a, contact pressure increase as the thread diameter and length increase. For 1 mm thread length, the tension suddenly increased when the installation was 1 mm, and for 2 mm long screws, the tension suddenly increased when the installation was 2 mm. This happens when the first thread is fully inserted into the screw hole. In other words, the contact pressure suddenly increased in the first step, where the thread was widest, and continued by reaching equilibrium in the following steps. In addition, it is clearly seen that the contact pressure increases as the thread length and width increase.

Figure 12b shows that, parallel to the contact pressures, the contact stresses increase as the thread length and width increase. Tension suddenly increased at 4 mm installation depth and returned to its previous state at the next installation depth in the samples with 2 mm thread length. This situation is explained as 2 threads steps increased the surface tension and as the other screw steps settle into the hole, it decreases as more area resists the tension.

Predictive expressions for mounting force and withdrawal strength

The mean mounting force and withdrawal strength were compared, and functional correlations between those forces and the different thread sizes for PB were determined through the use of multiple regression analysis (Equation 1, Equation 2).

$$Fm = 455{,}1 + 855 * TW - 199{,}8 * TL + 456 * TW * TL \quad (1)$$

$$Fw = 408{,}2 + 582 * TW - 29{,}1 * TL + 45 * TW * TL \quad (2)$$

Where Fm = mounting force; Fw = withdrawal strength; TW = thread widh; TL = thread length. The coefficients of determination (R2) values were obtained as 0,87 and 0,52 for mounting force and withdrawal strength, respectively.

Comparisons of the experimental results with the results obtained from the predictive expressions developed in this study are given in Table 5 in order to provide a practical assessment of whether the mounting force and withdrawal strength values predicted by these developed expressions agreed with the observed from experiments.

Table 5: Comparison of experimental mounting force and withdrawal strength mean values with the results obtained from predictive expressions.

Mounting Force				
Thread Width (mm)	Thread Length (mm)	Experimental (N)	Predicted (N)	Predicted/Experimental
0,2	1	509,03 (9,76)	515,50	1,01
	2	400,03 (7,99)	408,90	1,02
0,3	1	664,90 (11,30)	648,60	0,98
	2	602,33 (8,62)	585,60	0,97
0,4	1	771,07 (7,92)	779,70	1,01
	2	753,19 (4,02)	762,30	1,01
Withdrawal Strength				
Thread Width (mm)	Thread Length (mm)	Experimental (N)	Predicted (N)	Predicted/Experimental
0,2	1	482,87 (12,98)	504,50	1,04
	2	465,43 (9,43)	484,40	1,04
0,3	1	610,40 (7,72)	567,20	0,93
	2	589,58 (4,47)	551,60	0,94
0,4	1	608,22 (6,50)	629,90	1,04
	2	599,81 (7,21)	618,80	1,03

Values in the parenthesis are coefficients of variation.

According to Table 5, the worst prediction in the calculations made with the developed expressions was 0,97 and 0,93 for mounting force and withdrawal strength, respectively. Therefore, it could be said that the mounting force and withdrawal strength values of the STDs in PB can be reasonably predicted by using the Equation 1 and Equation 2.

CONCLUSIONS

This study was carried out to obtain experimental and numerical information relating to the mounting force and withdrawal strength of 3D printed PLA self-threaded dowels (STDs) connected with PB. Contact pressures and contact stresses was determined by using numerical analysis (FEM). Within the scope of the study, the mounting force and withdrawal strength of STDs with 3 different thread widths and 2 different thread lengths were tested in PB and predictive expressions were developed. Briefly, STDs that provide without glue connection and are easy to assemble were designed and developed, and their mechanical properties were examined experimentally and numerically.

According to the experimental results, the STDs with 0,2 mm thread width and 2 mm thread length gave the lowest mounting force, while the STDs with 0,4 mm thread width and 1 mm thread length gave the highest mounting force. In another words, increasing the thread width and decreasing the thread length of STDs increased the mounting forces. Referring to the withdrawal tests, the lowest average value was obtained from 0,2 mm width - 2 mm length thread. The highest withdrawal capacity was obtained from 0,4 mm width - 2 mm length thread. As shown in Figure 9, there is no significant difference between the withdrawal force capacity of the 0,3 mm and 0,4 mm width threads. In this context, considering the 3D printer production conditions, mounting forces and withdrawal force capacities, it has been determined that the most suitable thread size for STDs is 0,3 mm width - 2 mm length for particleboards.

According to numerical analysis of mounting force, the STD with 0,4 mm thread width had the highest contact stresses and contact pressure values. That results agree with the experimental test results. The STDs with 0,4 mm thread width had the highest value for the both mounting and withdrawal tests results. Furthermore, when mounting force, withdrawal strength and failure modes investigated; the STDs with 0,3 mm thread width determined as optimum thread width for this study. Additionally, the results show that for the withdrawal tests, the STDs with 0,4 mm thread width gave the highest value, while the STDs with 0,2 mm thread width gave the lowest value. There was no statistically significant difference between the withdrawal strength of STDs with 0,3 mm and 0,4 mm thread width. When the withdrawal strengths were examined, it was also seen that the thread length and two-way interaction were not statistically significant. When the mounting forces and withdrawal strengths of the STDs are evaluated together; according to the results of the study, the optimum STD is the one with 0,3 mm thread width and 2 mm thread length.

The other important finding came from comparing the predicted and experimental test results, which demonstrated that the mean mounting force and withdrawal strength of the STD examined in this study could be estimated utilizing developed predictive expressions. Accordingly, the mounting forces and withdrawal strengths of STDs with different thread widths and thread lengths can be predicted thanks to the formulas developed in this study.

The study can be expanded by using different thread geometries, different thread sizes and different composite materials. In this context, the future studies about fasteners without glue will both popularize the use of fasteners in composite materials and accelerate production processes. In addition, the use of these fasteners will facilitate the packaging and transportation of products. Producing easy to apply and inexpensive fasteners will also provide advantages for end users.

In addition, the study can be developed using different parameters of 3D printing and different production technologies (injection molded), different filaments and different composite materials.

Therefore, it can be recommended that in order to create STDs for future research, stronger materials can be used, or that alternative 3D printing techniques or injection molding systems can be tested. Also, that study can be extended by using other materials as wooden composites and solid wood.

Authorship contributions

T. K.: Conceptualization, Methodology, Validation, Formal Analysis, Investigation, Data Curation, Writing - Original Draft, Writing - Review & Editing, Visualization, Project Administration, Software, Funding Acquisition.

REFERENCES

ASTM. 2017. Standard Test Method for Tensile Properties of Polymer Matrix Composite Materials. ASTM D3039 / D3039M - 17.

Chen, M.; Li, X.; Lyu, J. 2018. Influence of Dowel Diameter and curing time on strength of double dowel joint. *Wood Research* 63(4): 591-598. http://www.woodresearch.sk/wr/201804/06.pdf

Chen, M.; Lyu, J.H.; Li, S.G.; Wu, X. 2017. Construction and implementation of a panel furniture design evaluation system at the design stage. *Advances in Mechanical Engineering* 9(2): 1-8. https://doi.org/10.1177/1687814017693945

Dassault Systèmes Simulia Corp. 2013. Abaqus/Explicit v.6.13-1. Waltham, MA, USA. https://www.3ds.com/products/simulia/abaqus.

Gross, B.C.; Erkal, J.L.; Lockwood, S.Y.; Chen, C.; Spence, D.M. 2014. Evaluation of 3D Printing and Its Potential Impact on Biotechnology and the Chemical Sciences. *Analytical Chemistry* 86(7): 3240-3253. https://doi.org/10.1021/ac403397r

Hajdarević, S.; Martinović, S. 2014. Effect of tenon length on flexibility of mortise and tenon joint. *Procedia Engineering* 69: 678-685. https://doi.org/10.1016/j.proeng.2014.03.042

Hao, J.; Xu, L.; Wu, X.; Li, X. 2020. Analysis and modeling of the dowel connection in wood T type joint for optimal performance. *Composite Structures* 253: e112754. https://doi.org/10.1016/j.compstruct.2020.112754

Ho, C.M.B.; Ng, S.H.; Yoon, Y. J. 2015. A review on 3D printed bioimplants. *International Journal of Precision Engineering and Manufacturing* 16(5): 1035-1046. https://doi.org/10.1007/s12541-015-0134-x

Kasal, A.; Smardzewski, J.; Kuskun, T.; Erdil, Y. Z.2016. Numerical analyses of various sizes of mortise and tenon furniture joints. *BioResources* 11(3): 6836-6853. https://doi.org/10.15376/biores.11.3.6836-6853

Kuşkun, T.; Smardzewski, J.; Kasal, A. 2021. Experimental and numerical analysis of mounting force of auxetic dowels for furniture joints. *Engineering Structures* 226: e111351. https://doi.org/10.1016/j.engstruct.2020.111351

Lin, L.; Fang, Y.; Liao, Y.; Chen, G.; Gao, C.; Zhu, P. 2019. 3D Printing and Digital Processing Techniques in Dentistry: A Review of Literature. *Advanced Engineering Materials* 21(6): e1801013. https://doi.org/10.1002/adem.201801013

Lukic, M.; Clarke, J.; Tuck, C.; Whittow, W.; Wells, G. 2016. Printability of elastomer latex for additive manufacturing or 3D printing. *Journal of Applied Polymer Science* 133: e42931. https://doi.org/10.1002/app.42931

Minitab. 2023. Minitab Statistical Software, versión 17.1. Minitab, LLC: State College, PA, USA. https://www.minitab.com/en-us/

Mougel, E.; Segovia, C.; Pizzi, A.; Thomas, A. 2011. Shrink-Fitting and Dowel Welding in Mortise and Tenon Structural Wood Joints. *Journal of Adhesion Science and Technology* 25(1-3): 213-221. https://doi.org/10.1163/016942410X503320

Norvydas, V.Ė; Juodeikienė, I.; Minelga, D. 2005. The Influence of Glued Dowel Joints Construction on the Bending Moment Resistance. *Journal of Materials Science* 11(1): 36-39. https://matsc.ktu.lt/index.php/MatSc/article/view/26484

Park, H.J.; Semple, K.; Smith, G.D. 2006. Screw thread shape and fastener type effects on load capacities of screw-based particleboard joints in case construction. *Forest Products Journal* 56(4): 48-55. https://link.gale.com/apps/doc/A145832718/AONE?u=anon~fb83c5e6&sid=googleScholar&xid=a69c0c85

Sawata, K.; Yasumura, M. 2002. Determination of embedding strength of wood for dowel-type fasteners. *Journal of Wood Science* 48(2): 138-146. https://doi.org/10.1007/BF00767291

Smardzewski, J.; Ozarska, B. 2005. Rigidity of Cabinet Furniture with Semi-Rigid Joints of the Confirmat Type. *Electronic Journal of Polish Agricultural Universities* 8(2): 1-12. http://www.ejpau.media.pl/articles/volume8/issue2/art-32.pdf

Su, A.; Al'Aref, S.J. 2018. History of 3D printing. In: *3D Printing Applications in Cardiovascular Medicine*. Al'Aref, S.J.; Mosadegh, B.; Dunham, S.; Min, J.K. Academic Press Elsevier Inc.: Boston, USA. https://doi.org/10.1016/B978-0-12-803917-5.00001-8

Vukicevic, M.; Mosadegh, B.; Min, J. K.; Little, S. H. 2017. Cardiac 3D Printing and its Future Directions. *JACC: Cardiovascular Imaging* 10(2): 171-184. https://doi.org/10.1016/j.jcmg.2016.12.001

Wang, Y.; Lee, S.H. 2014. Design and analysis on interference fit in the hardwood dowelglued joint by finite element method. *Procedia Engineering* 79: 166-172. https://doi.org/10.1016/j.proeng.2014.06.326

Yüksel, M.; Kılıç, H.; Kuşkun, T.; Kasal, A. 2022. Predictive Expressions for Withdrawal Force Capacity of Various Size of Dowels From Particleboard and Medium Density Fiberboard. *Maderas. Ciencia y Tecnología* (24): 1-16. https://doi.org/10.4067/s0718-221x2022000100436

Zhang, C.; Chang, W.S.; Harris, R. 2016. Investigation of thread configuration of self-tapping screws as reinforcement for dowel-type connection. In World Conference on Timber Engineering, WCTE. 22-25 agosto. Vienna, Austria. https://researchportal.bath.ac.uk/en/publications/investigation-of-thread-configuration-of-self-tapping-screws-as-r

Zhang, J.; Eckelman, C.A. 1993. The bending moment resistance of single-dowel corner joints in case construction. *Forest Products Journal* 43(6): 19-24. https://www.proquest.com/scholarly-journals/bending-moment-resistance-single-dowel-corner/docview/214634085/se-2